

We are IntechOpen, the world's leading publisher of Open Access books Built by scientists, for scientists

6,900

Open access books available

186,000

International authors and editors

200M

Downloads

Our authors are among the

154

Countries delivered to

TOP 1%

most cited scientists

12.2%

Contributors from top 500 universities



WEB OF SCIENCE™

Selection of our books indexed in the Book Citation Index
in Web of Science™ Core Collection (BKCI)

Interested in publishing with us?
Contact book.department@intechopen.com

Numbers displayed above are based on latest data collected.
For more information visit www.intechopen.com



Potentiometric Determination of Ion-Pair Formation Constants of Crown Ether-Complex Ions with Some Pairing Anions in Water Using Commercial Ion-Selective Electrodes

Yoshihiro Kudo

Additional information is available at the end of the chapter

<http://dx.doi.org/10.5772/48206>

1. Introduction

Ion-pair formation equilibrium-constants or association ones in water have been determined so far using various methods. As representative methods, one can suppose conductometry, spectrophotometry [1], potentiometry [1], voltammetry [2], calorimetry, electrophoresis [3], and so on. The conductometric measurements generally have high accuracies for their determination for metal salts (MX_z at $z = 1, 2$) and of their metal complex-ions (ML^{z+}) with pairing anions (X^{z-}) in water and in pure organic solvents. According to our knowledge, its experimental operation requires high experimental know-how to handle the measurements. Also, the spectrophotometric measurements require the condition that either species formed in or those consumed in the ion-pair formation are of colored at least. Solvent extraction methods are generally difficult to establish some experimental conditions, such as ionic strength (I) of both phases and solvent compositions, compared with the above two methods. Strictly speaking, its constants are hard to recognize as thermodynamic ones.

We treat here the ion-pair formation of crown compounds (L), such as 15-crown-5 and 18-crown-6 ethers (15C5 and 18C6), with colorless alkali, alkaline-earth metal ions, and so on in water [4-8]. The methods described above are difficult to apply for the determination of the constants. For example, conductometry cannot distinguish among the metal ions M^{z+} , their ML^{z+} , and X^{z-} in water and ML^{z+} is unstable in many cases. Also, many M^{z+} and ML^{z+} employed here cannot be detected spectrophotometrically. Voltammetric methods cannot apply for the determination, because working electrode suitable for M^{z+} detection is difficult to get. While, polarography with DME can be effective for the measurements of such

systems [2]. Unfortunately, it must use mercury and its salts which pollute the environment around us.

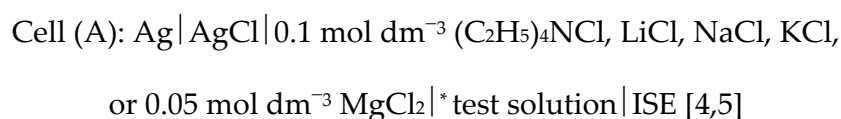
Thus, in order to overcome these limitations, potentiometry with ISE has been applied for the determination of the ion-pair formation constants ($K_{MLX_z^0}$) for MLX_z in water at $I \rightarrow 0$ mol dm^{-3} , although its applications are limited by kinds of commercial ISE. In the present chapter, its fundamentals and applications for the formation systems of MX_z and MLX_z in water are described. Here, the determination of $K_{MX_z^0}$, the ion-pair formation constant of MX_z in water at $I \rightarrow 0$, is always required for that of $K_{MLX_z^0}$.

2. Emf measurements

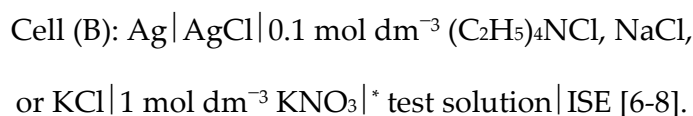
2.1. Electrochemical cells [4-8]

Constitutions of cells employed for emf measurements of test solutions are described as follows.

As a cell with a single liquid junction



or as that with a double liquid junction



Here, the 1 mol dm^{-3} solution of KNO_3 in Cell (B) is a salt bridge, between which and the test solution, E_j estimated from the Henderson equation [2] is in the range of 1 to 3 mV in many cases [9]. Standard types for the reference electrodes of Cells (A) and (B) are $\text{Ag} | \text{AgCl} | 0.1 \text{ mol dm}^{-3} (\text{C}_2\text{H}_5)_4\text{NCl}$ and $\text{Ag} | \text{AgCl} | 0.1 \text{ mol dm}^{-3} \text{ KCl} | 1 \text{ mol dm}^{-3} \text{ KNO}_3$, respectively. For Cell (A), the E_j values are corrected by the Henderson equation {see Eq. (1)}, while they are not corrected for Cell (B).

2.1.1. For ion-selective electrodes

Commercial ISEs used here are summarized in Table 1 and some comments for the present emf measurements are described.

2.1.2. Corrections of liquid junction potentials [2]

For emf measurements of the electrochemical cells, the problem of the liquid junction potentials E_j occurred at the interface marked with an asterisk cannot be avoided. Hence, correction procedures of E_j are described in this section. Here, the salt bridges with KNO_3 are experimentally used and the Henderson equation [2]

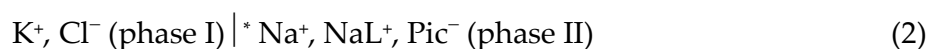
ISE	Type & Maker	Comments
Na ⁺ -selective electrode	1512A-10C, Horiba	Glass membrane; this electrode partially responds K ⁺ and Rb ⁺ .
K ⁺ -selective electrodes	1200K, Toko	Glass membrane (not produced now); this electrode partially responded Li ⁺ .
	8202-10C, Horiba	Liquid membrane; it is unstable for the aqueous solution of hydrophobic picrates.
Ag ⁺ -selective electrode	8011-10C, Horiba	Solid membrane
Cd ²⁺ -selective electrode	8007-10C, Horiba	Solid membrane; it responds Br ⁻ partially and I ⁻ well. See below.
Cl ⁻ -selective electrode	8002-10C, Horiba	Solid membrane
Br ⁻ -selective electrode	8005-10C, Horiba	Solid membrane
I ⁻ -selective electrode	8004-10C, Horiba	Solid membrane

a. The above ISEs are used with a Ag|AgCl reference electrodes, Horiba, types 2660A-10T (single junction type) and 2565A-10T (double junction one).

Table 1. Commercial ISEs used here^a

$$E_j = \phi^{\text{II}} - \phi^{\text{I}} = - \frac{\sum_j |z_j| \frac{u_j}{z_j} (c_j^{\text{II}} - c_j^{\text{I}})}{\sum_j |z_j| u_j (c_j^{\text{II}} - c_j^{\text{I}})} \frac{RT}{F} \ln \frac{\sum_j |z_j| u_j c_j^{\text{II}}}{\sum_j |z_j| u_j c_j^{\text{I}}} \quad (1)$$

is analytically employed for the correction of E_j . For example, the molar concentration of j in the phase I, c_j^{I} , consists of $c_{\text{K}^{\text{I}}}$ and $c_{\text{Cl}^{\text{I}}}$, while c_j^{II} does of $c_{\text{Na}^{\text{II}}}$, $c_{\text{NaL}^{\text{II}}}$, and $c_{\text{Pic}^{\text{II}}}$ for the NaPic-L system, where ions involved in a part of the cell are expressed as



(see the case 1L). Also, the $u_{\text{Na}^{\text{II}}} + u_{\text{NaL}^{\text{II}}}$ term in Eq. (1) can be assumed to be $u_{\text{Na}}(c_{\text{Na}^{\text{II}}} + c_{\text{NaL}^{\text{II}}})$ in practice (see Table 2 for the u_{Na} value), because the condition of $c_{\text{Na}^{\text{II}}} \gg u_{\text{NaL}^{\text{II}}}/u_{\text{Na}}$ holds in many cases with L (low stabilities of ML^{z^+} in water).

2.2. Emf measurements

2.2.1. Preparation of calibration curves

A representative procedure for preparing a calibration curve is described below. Using a pipette, 55 cm³ of the aqueous solution of NaCl or KCl is precisely prepared in 100 cm³ beaker, kept at 25 ± 0.3 or 0.4 °C, and then slowly stirred with a Teflon bar containing a magnet. To this solution, the ISE corresponding to Na⁺ or K⁺ and the reference electrode are immersed. A 7 or 10 cm³ portion of pure water is added by the pipette and, after 5 minutes, emf values at a steady state are read. This operation is repeated, when the amount of the

solution is reached to about 100 cm³. Consequently, 7 or 5 data are obtained in a unit operation. The thus-obtained calibration curves are shown in Fig. 1.

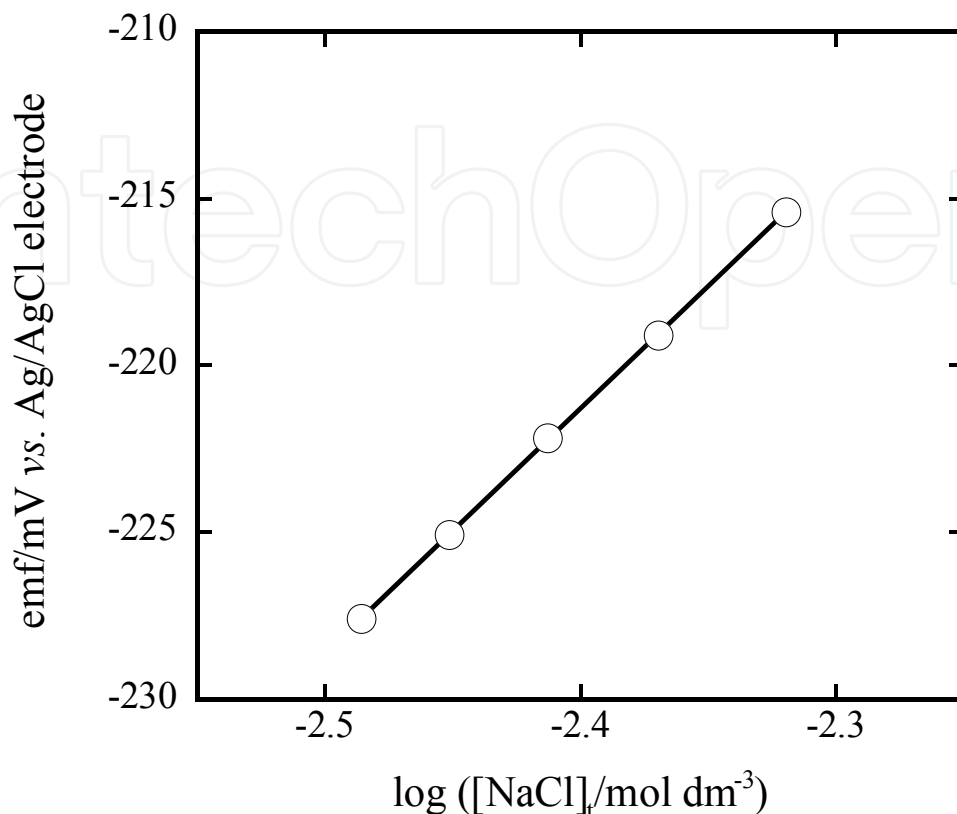


Figure 1. Calibration curve of aqueous NaCl solution at 25 °C. $\text{Emf} = 55.0 \log [\text{NaCl}]_t - 89.4$ at $R = 0.999$. This slope is close to 59 mV/decade, showing the Nernstian response with $z = 1$

A high-purity NaCl (99.98 to 99.99%) is dried about 160 °C in an oven [12]. The purities of other standards are checked by AgNO₃ titration for which the Ag⁺ solution is standardized with the high-purity NaCl.

2.2.2. Emf measurements of test solutions

A representative procedure for the emf measurements of the test solution is described here. Using a pipette, 55 cm³ of aqueous solution of MX_z is precisely prepared in 100 cm³ beaker, kept at 25 ± 0.3 or 0.4 °C, and then stirred with the Teflon bar. To this solution, the ISE and the reference electrode are immersed. A 7 or 10 cm³ portion of the aqueous solution of L (or pure water for the K_{MX_z} determination) is added by a pipette and after 5 minutes, emf values at a steady state are read. This operation is repeated, when the amount of the solution is reached to about 100 cm³. Consequently, 7 or 5 data are obtained in a unit operation. Then an example for the plot is shown with that of the corresponding calibration curve of the CdSO₄-18C6 system (Fig. 2). These plots indicate that [Cd²⁺] << [CdSO₄]_t in mixtures, compared with the calibration curve depicted at open circles. All the above experiments are performed under the condition of [MX_z]_t ≈ [L]_t.

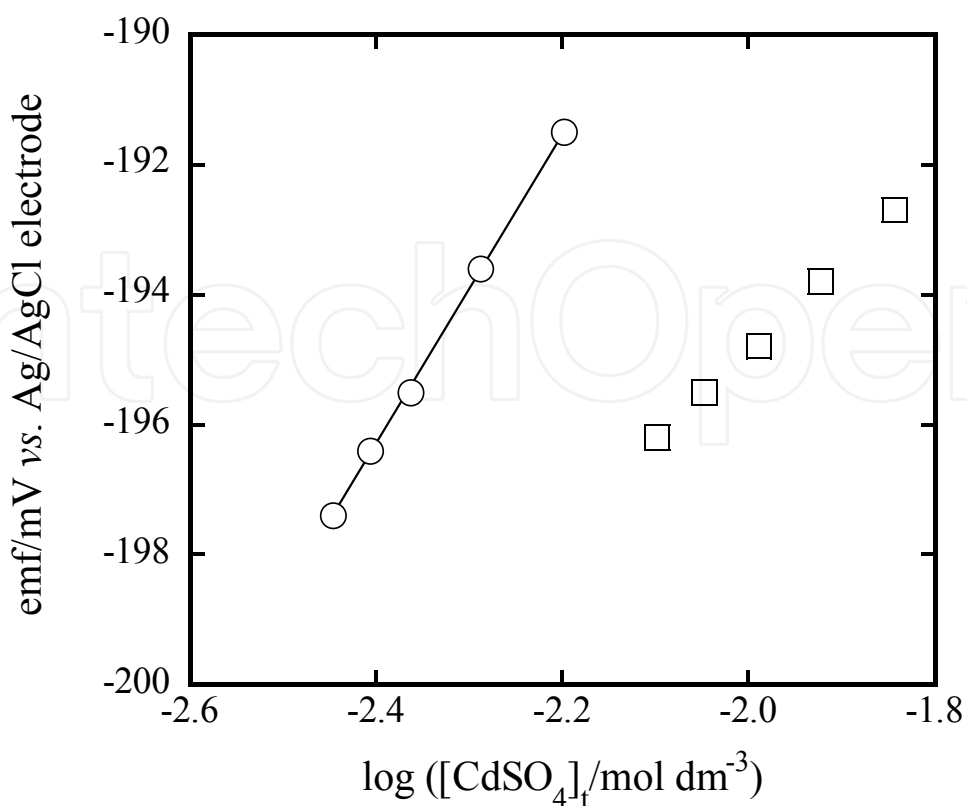


Figure 2. Calibration curve (open circles) of aqueous CdSO_4 solution at 25 °C. $\text{Emf} = 23.8 \log [\text{CdSO}_4]_t - 89.4$ at $R = 0.999$. This slope is close to 30 mV/decade, showing the Nernstian response with $z = 2$. Open squares show plots of mixtures of CdSO_4 with 18C6 in water at 25 °C.

3. Theoretical treatments and data analysis

3.1. Fundamentals

3.1.1. Ionic activity coefficients [10,13]

In order to determine the ion-pair formation constants at $I \rightarrow 0$ and 25 °C, the ionic activity coefficients (y_j) of ionic species j used for the activity (a_j) calculations are evaluated from the extended Debye-Hückel equation

$$\log y_j = -\frac{0.5114z_j^2\sqrt{I}}{1 + 0.3291a\sqrt{I}} \quad (3)$$

and the Davies one [13]

$$\log y_j = -0.5114z_j^2 \left(\frac{\sqrt{I}}{1 + \sqrt{I}} - 0.3I \right), \quad (4)$$

where a denotes the ion size parameter (see Table 2). In general, it is mentioned that the former equation is employed in the range of less than 0.1 mol dm^{-3} , while the latter one is done in that

of less than about 1 mol dm^{-3} . Also, the Davies equation can be used for some ions, such as ML^{z+} and $\text{M}^{\text{II}}\text{X}^+$, or for the y_j calculations of species j , of which the ion size parameters (e.g., DDTC^- , tfa^-) are not available, because its equation does not involve the parameter a . However, the accuracy of its y_j will be less than that of Eq. (3). The ion size parameters of some ions in water are listed in Table 2, together with their mobility data [11] at 25°C .

j	$a(j) / \text{\AA}$	$u_j / 10^{-4}$	j	$a(j) / \text{\AA}$	$u_j / 10^{-4}$
H^+	9	36.25	Cl^-	3	7.912
Li^+	6	4.010	Br^-	3	8.13
Na^+	4	5.193	I^-	3	7.96
K^+	3	7.619	NO_3^-	3	7.404
Ag^+	2.5	6.41 ₅	MnO_4^-	3.5	6.35
Ca^{2+}	6	6.166	ReO_4^-	3.9 ^c	5.69 ₇
Cd^{2+}	5	5.6	ClO_4^-	3.5	7.05
CdCl^+	4	--- ^d	Pic^-	7	3.149
$(\text{C}_2\text{H}_5)_4\text{N}^+$	6	3.38 ₄	BPh_4^-	9 ^c	2.2
			SO_4^{2-}	4	8.27
			$\text{S}_2\text{O}_3^{2-}$	4	8.81
			CrO_4^{2-}	4	8.8

a. Ref. [10].

b. $\text{cm}^2 \text{s}^{-1} \text{V}^{-1}$ unit. Calculated from ionic conductivity data. See Refs. [2] and [11].

c. Calculated from the Brüll formula. See Ref. [10].

d. Not be available.

Table 2. Ion size parameters^a and mobilities^b of some ions in water at 25°C

3.1.2. Model of ion-pair formation equilibria in water [4,6-8,12]

We introduce here three kinds of chemical equilibria for the ion-pair formation of single MX , MX_2 , and M_2X and their mixtures with L , except for chemical ones for the mixture of M_2X with L .

Case (1). 1:1 and 2:2 electrolytes



Case (2). 2:1 electrolytes

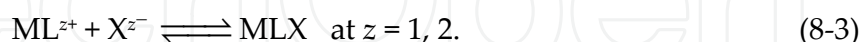


Case (3). 1:2 electrolytes





Case (1L). 1:1 or 2:2 electrolytes with L



Case (2L). 2:1 electrolytes with L



Ion-pair formation of M^+ or X^{2-} for Case (3) is omitted, because an example for the ion-pair formation of ML^+ with X^{2-} was not found for the present experiments. First, one determine the formation constants for Case (1) or (2) and next do those for Case (1L) or (2L), using the equilibrium constants determined by analyzing Case (1) or (2), respectively. Therefore, as you know, the experimental errors of the K values obtainable from Cases (1) and (2) become influenced those in the K determination of Cases (1L) and (2L), respectively (see Table 5).

3.2. Theoretical treatments and data analysis for Case (1) [4]

Analytical equations are derived from the models represented in the section 3.1.2. Using these equations, analytical procedures are described for the cases of the metal salts MX , M_2X , MX_2 , and their mixtures with L, except for those of M_2X with L. Here, M^{z+} and X^{z-} at $z = 1$ and 2 denote a metal ion and a pairing (or counter) anion, respectively.

3.2.1. Mass and charge balances and the theoretical treatments

To solve the above equilibria, mass- and charge-balance equations are shown. As an example, Case (1) is described as follows [4].

$$[MX]_t = [M^+] + [MX] + b_s \text{ for the species with } M^+ \quad (10)$$

$$[MX]_t = [X^-] + [MX] + b_s \text{ for those with } X^- \quad (11)$$

$$\text{and } [M^+] = [X^-] \quad (12)$$

For Case (1), its ion-pair formation constant (K_{MX}) in molar concentration unit is defined as

$$K_{MX} = y_M y_X K_{MX}^0 = \frac{[MX]}{[M^+][X^-]} \quad (y_{MX} = 1) \quad (13)$$

Considering an apparent total concentration to be $[MX]_t - b_s$, one can express $[MX]$ and $[X^-]$ as functions of $[M^+]$. Thus, taking logarithms of the both sides of Eq. (13) and rearranging its equation, the following one is obtained.

$$\log \frac{K_{MX}}{y_{\pm}^2} = \log \left(K_{MX}^0 + \frac{b_s}{a_M^2} \right) \quad (14)$$

$$\text{with } y_{\pm} = \sqrt{y_+ y_-} \quad (14-1)$$

$$\text{and } K_{MX} = ([MX]_t - [M^+])/[M^+]^2. \quad (14-2)$$

When the $[M^+]$ value is determined with ISE, then Eq. (14-2) is easily obtained at a given I .

3.2.2. Data analysis [4]

Hence, one can plot $\log (K_{MX}/y_{\pm}^2)$ against a_M^2 and immediately obtain the K_{MX}^0 and b_s values (mol dm⁻³ unit) from analyzing its plot by a non-linear regression. Figure 3 shows the plot for the NaPic system at 25 °C [4]. Table 3 lists the analytical equations for the other cases, together with equations expressing I which are derived from the charge-balance equations. Also, details for calculation of the parameters listed in Table 3 are summarized in Table 4 [4,6,8,12].

Case	Equation for analysis	Plot for analysis	I / mol dm ⁻³
(1)	$\log \frac{K_{MX}}{y_{\pm}^2} = \log \left(K_{MX}^0 + \frac{b_s}{a_M^2} \right) \text{ at } z = 1, 2;$ $b_s/\text{mol dm}^{-3}: \text{curve-fitting parameter}$	$\log (K_{MX}/y_{\pm}^2)$ <i>versus</i> a_M^2	$[M^+]$ or $[X^-]$
(2)	$\sum a_j/a_M = 1 + K_1^0 a_X + K_1^0 K_2^0 (a_X)^2$	$\sum a_j/a_M$ <i>versus</i> a_X	$[M^{2+}] + [X^-]$
(3)	$\sum a_j/a_X = 1 + K_1^0 a_M + K_1^0 K_2^0 (a_M)^2$	$\sum a_j/a_X$ <i>versus</i> a_M	$[M^+] + [X^{2-}]$
(1L)	$\log \frac{K_{MLX}}{y_{\pm}^2} = \log \left(K_{MLX}^0 + \frac{b_c}{y_{ML}([X^-] - [M^+])a_X} \right) \text{ at } z = 1;$ $b_c/\text{mol dm}^{-3}: \text{curve-fitting parameter}$	$\log (K_{MLX}/y_{\pm}^2)$ <i>versus</i> $y_{ML}([X^-] - [M^+])a_X$	$[X^-]$
(2L)	$F(a_j) \approx 1 + K_{MLX}^0 a_X + K_{MLX}^0 K_{MLX2}^0 (a_X)^2$ $\text{with } F(a_j) = \frac{\sum a_j - a_M(1 + K_{MX}^0 a_X)}{a_{ML}}$	$F(a_j)$ <i>versus</i> a_X	$[M^{2+}] + [ML^{2+}] + [X^-]$

Table 3. Equations and plots for the equilibrium analyses and I expressions corresponding to them [4,6,8,12]

Case	Molar concentrations of respective species at equilibrium	Remarks
(1)	$[M^{z+}]$ or $[X^{z-}]$: analyzed for $z = 1, 2$	Ref. [4]
(3)	$[M^+]$: analyzed; $[X^{2-}] = \frac{[M^+]}{2 + K_{MX}[M^+]}$; $[MX^-] = \frac{K_{MX}[M^+]^2}{2 + K_{MX}[M^+]}$; $[M_2X] = [M_2X]_t - \frac{[M^+](1 + K_{MX}[M^+])}{2 + K_{MX}[M^+]}$, where $K_{MX} = [MX^-]/[M^+][X^{2-}]$	Ref. [12]
(1L)	$[M^{z+}]$: analyzed; $[X^{z-}] = \frac{[M^{z+}](1 + K_{ML}[M^{z+}])}{1 - K_{ML}K_{MX}[M^{z+}]}$; $[ML^{z+}] = [X^{z-}] - [M^{z+}]$; $[MLX] = [MX]_t - [X^{z-}](1 + K_{MX}[M^{z+}])$, where $K_{MX} = [MX]/[M^{z+}][X^{z-}]$ for $z = 1, 2$	Ref. [4]
(2L)	$[X^-]$: analyzed; $[M^{2+}] = \frac{[MX_2]_t - \sum[MLX_z]}{1 + K_{MX}[X^-] + K_{ML}[L]}$; $[L] = \frac{[L]_t - \sum[MLX_z]}{1 + K_{ML}[M^{2+}]}$; $\sum[MLX_z] = [MX_2]_t - [M^{2+}](1 + K_{MX}[X^-] + K_{ML}[L])$, where $K_{MX} = [MX]/[M^{2+}][X^-]$	One can compute $[M^{2+}]$, $[L]$, and $\sum[MLX_z]$ by a successive approximation. See Ref. [8] for its details.

a. Equations correspond to Cases in Table 3. See the text for Case (2)

Table 4. Equations and plots for the equilibrium analyses and I expressions corresponding to them [4,6,8,12]

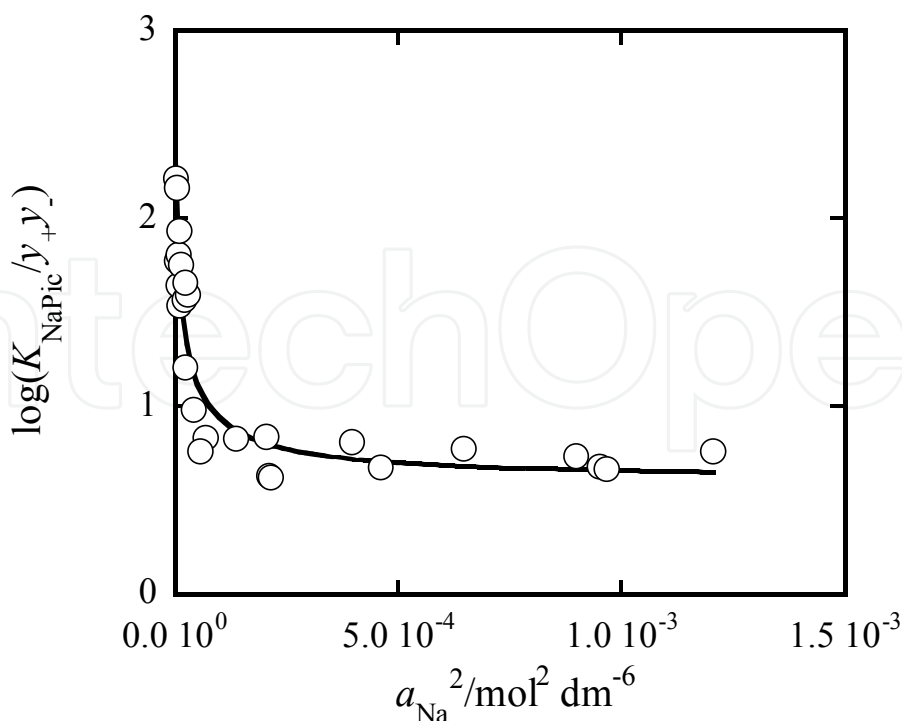


Figure 3. Plot of $\log(K_{NaPic}/y_{\pm}^2)$ versus a_{Na^2} with $b_s = 5.3 \times 10^{-4} \text{ mol dm}^{-3}$ and $R = 0.945$ [4].

3.2.3. 2:2 electrolytes [6]

Table 3 lists the equation [6] for the equilibrium analysis and the parameters for its analytical plot corresponding to Case (1) at $z = 2$. Similarly, the equations for the calculation of the parameters and equilibrium constants are summarized in Table 4.

3.3. Theoretical treatments and data analysis for Case (2) [12]

From the mass- and charge-balance equations [12] of Case (2), the following equations are derived.

$$[X^-] = \frac{2[M^{2+}]}{1 - K_{MX}[M^{2+}]} \text{ for } M^{2+} \text{ determination by ISE} \quad (15)$$

or

$$[M^{2+}] = \frac{[X^-]}{2 + K_{MX}[X^-]} \text{ for } X^- \text{ determination by ISE} \quad (16)$$

The concentrations of other species are

$$[MX^+] = \frac{2K_{MX}[M^{2+}]^2}{1 - K_{MX}[M^{2+}]} \quad (17)$$

and

$$[MX_2] = [MX_2]_t - \frac{[M^{2+}](1 + K_{MX}[M^{2+}]^2)}{1 - K_{MX}[M^{2+}]} \quad (18)$$

On the basis of the above equations, one can immediately calculate $K_{MX} = [MX^+]/[M^{2+}][X^-]$ and $K_2 = [MX_2]/[MX^+][X^-]$ for a given I . For the other cases, see Tables 3 and 4. As an example, the plot of the Na_2CrO_4 system is shown in Fig. 4. Also, Table 5 lists the K_{MX}^0 and K_2^0 values determined in the section 3.2 and the present one [4-8,12,14].

3.4. HSAB principle [15,16]

According to Pearson, the HSAB classifications of some species are as follows.

As hard acids: H^+ , Li^+ , Na^+ , K^+ , Ca^{2+} , Sr^{2+} etc.

As borderline acids: Fe^{2+} , Co^{2+} , Ni^{2+} , Cu^{2+} , Zn^{2+} , Pb^{2+} etc.

As soft acids: Ag^+ , Tl^+ , Pd^{2+} , Cd^{2+} , Hg^{2+} etc.

and

As hard bases: H_2O , OH^- , F^- , PO_4^{3-} , SO_4^{2-} , Cl^- , ClO_4^- , ROH , RO^- , R_2O etc.

As borderline bases: N_3^- , Br^- , NO_2^- , SO_3^- , N_2 etc.

As soft bases: R_2S , RSH , RS^- , I^- , SCN^- , CN^- etc. with R = aryl or alkyl group

These species are best classified by using the following criteria. Class (a) acids (hard ones) form more stable complexes with ligands having the Y donor atoms in the order $\text{Y} = \text{N} \gg \text{P} > \text{As} > \text{Sb}$; $\text{O} \gg \text{S} > \text{Se} > \text{Te}$; $\text{F} > \text{Cl} > \text{Br} > \text{I}$ [15]. On the other hand, Class (b) acids (soft ones) form in the order $\text{N} \ll \text{P} > \text{As} > \text{Sb}$; $\text{O} \ll \text{S} < \text{Se} \sim \text{Te}$; $\text{F} < \text{Cl} < \text{Br} < \text{I}$ [15]. So, what criteria do ML^{z+} classify? What criteria do L classify? For some ions and crown ethers, these HSAB classifications are going to be examined below (see 4.2) on the basis of the K_{MX^0} and K_{MLX^0} values at $z = 1$ and 2.

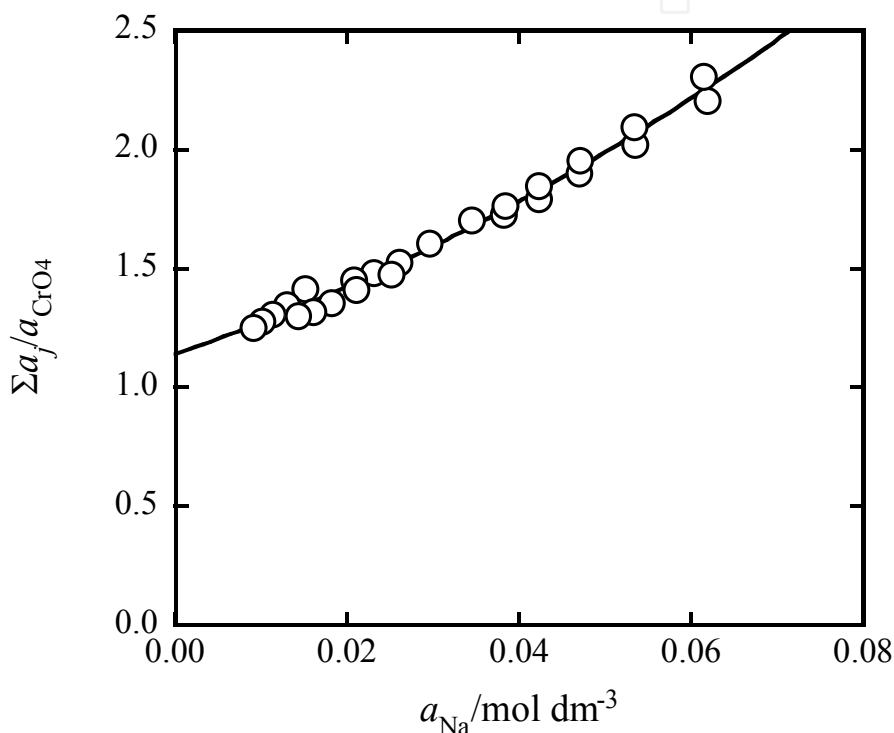


Figure 4. Plot of $\Sigma a_j / a_{\text{CrO}_4}$ versus a_{Na} with $R = 0.994$

3.5. Theoretical treatments and data analysis for mixtures with L

3.5.1. For Cases (1L) and (2L) [4,8]

As similar to the section 3.2, Table 3 summarizes the analytical equations and their plot types. Examples of the plots for Cases (1L) and (2L) are shown in Figs. 5 and 6, respectively. The plot in Fig. 5 is similar to that in Fig. 3. A fitting curve of $\log (K_{\text{MLX}}/y_{\pm}^2)$ versus a_{MLX} is depicted with a solid line in Fig. 5, where $a_{\text{ML}} = y_{\text{ML}}([\text{X}^-] - [\text{M}^+])$ [4]. The former parameter obviously corresponds to $\log (K_{\text{MX}}/y_{\pm}^2)$ in Case (1) and the latter one to a_{M^2} {see the section 3.2.1. Table 5 lists the K_{MLX^0} (and β_2^0) values thus determined at 25 °C. From this table, one can easily see that the K_{MLX^0} values are larger than the K_{MX^0} ones, except for several cases. These results indicate that M^{z+} dehydrates in the complex formation with L in water and thereby increases its hydrophobic property.

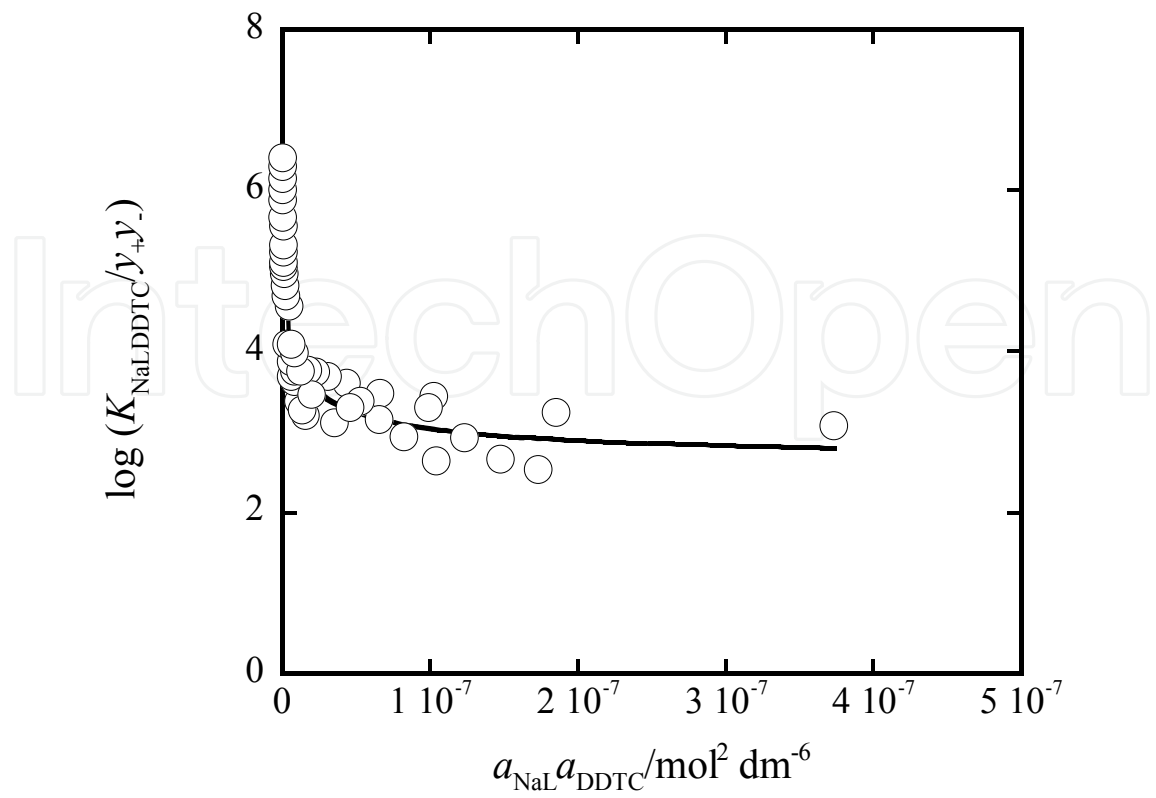


Figure 5. Plot of $\log(K_{\text{NaLDDTC}}/y_{\pm}^2)$ versus $a_{\text{NaL}} a_{\text{DDTC}}$ with $R = 0.973$ for L = 15C5.

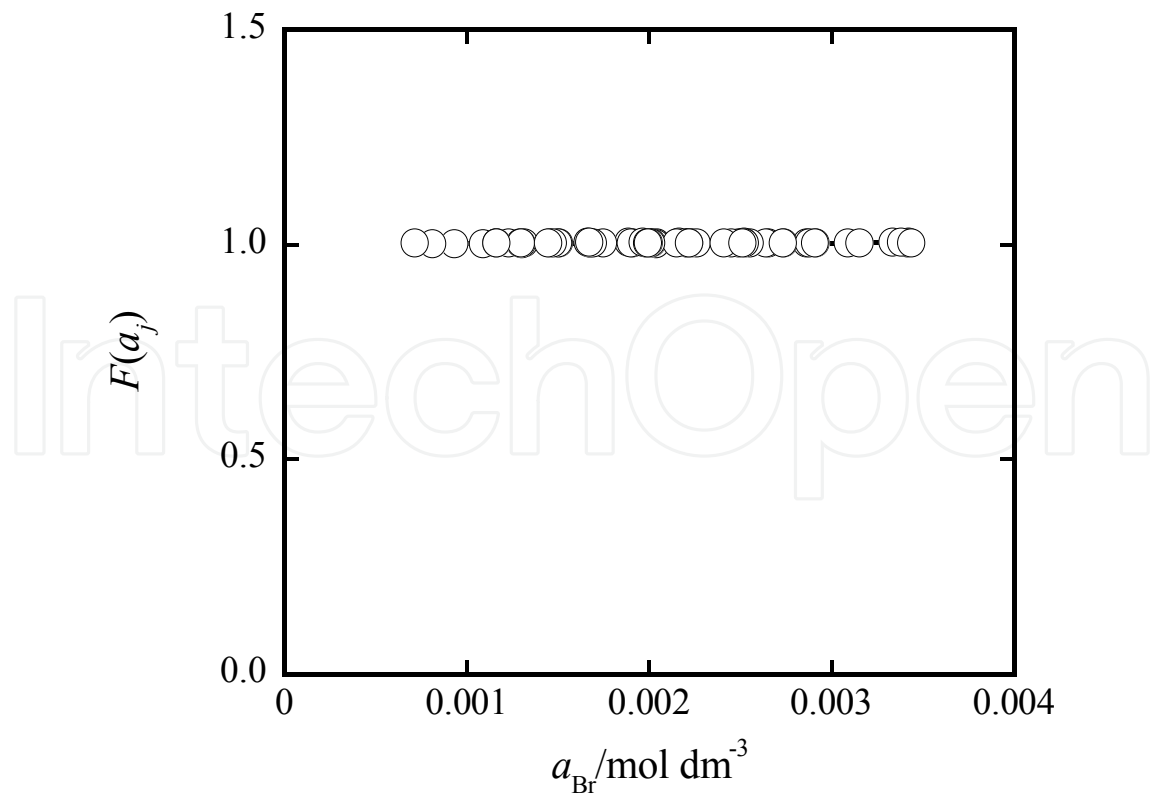


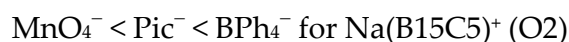
Figure 6. Plot of $F(a_j)$ versus a_{Br} with $R = 0.484$ for the CdBr_2 -18C6 system.

4. Ion-pair formation for MX_z with L in water

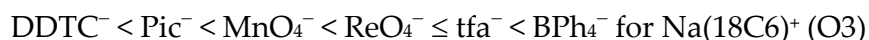
4.1. Dependence of the ion-pair formation constants on some factors [4-8]

4.1.1. Effect of sizes of anions

Effect of sizes of anions X^{z-} on the K_{MLX}^0 values is described and thereby its cause is examined. Effective ionic radii or sizes estimated from the Van der Waals (vdw) volumes are on the order $\text{X}^{z-} = \text{Cl}^- < \text{Br}^- < \text{tfa}^-$ (estimated from vdw vol.) $\leq \text{I}^- < \text{MnO}_4^- < \text{ReO}_4^- < \text{DDTC}^-$ (from vdw vol.) $< (\text{SO}_4^{2-} <) \text{Pic}^- < \text{BPh}_4^-$ [8]. The K_{MLX}^0 values in Table 5 are on the orders



and



The two orders, (O1) and (O2), suggest hydrophobic interactions between BPh_4^- and Na(15C5)^+ or Na(B15C5)^+ and those between Pic^- and Na(B15C5)^+ . That is, the former two cases reflect the interaction between the large ions, while the latter case does that between a benzene ring in Pic^- and a benzo group in Na(B15C5)^+ . Other K_{MLX}^0 orders seem to have the characteristics that $\text{DDTC}^- \ll \text{BPh}_4^-$ (is due to the hydrophobic interaction), $\text{Pic}^- < \text{MnO}_4^-$, and $\text{ReO}_4^- \leq \text{tfa}^-$ (are due to the electrostatic one).

4.1.2. Effect of a benzo group added to L skeleton

Effect of a benzo group of L on the K_{MLX}^0 values is described and thereby its cause is discussed. Table 5 reveals relations



and



Considering the electrostatic interaction between ML^+ and X^- and water molecules hydrated to M^+ to be basic interactions, these relations of Inequalities (R5) to (R8) may be changed into the following expression: $\text{Na}^+(15\text{C5})^- \leq (\text{B15C5})\text{Na}^+-\text{X}^-$ and $w\text{Ag}^+(15\text{C5})^- \leq (\text{B15C5})\text{Ag}^+-\text{Pic}^-$ for Inequality (R5); $(15\text{C5})\text{K}^+w^- > w\text{K}^+(\text{B15C5})-\text{X}^-$ for (R6) and $w\text{Na}^+(18\text{C6})^- < (\text{B18C6})\text{Na}^+-\text{X}^-$

and $K^+(18C6)^- < (B18C6)K^+-Pic^-$ for (R7); $(18C6)K^+ \geq K^+(B18C6)-MnO_4^-$ and $(18C6)M^+w^- \geq M^+(B18C6)-X^-$ for (R8). Here, w denotes the water molecules which hydrate to M^+ and act as Lewis base. Also, we simply define the following sequence

$$wM^+L-X^- < M^+L-X^- < LM^+w-X^- < LM^+-X^- \quad (SO9)$$

as a measure for the strength of the interaction between ML^{z+} and X^{z-} at $z = 1$. In other words, the standard order (SO9) can be interpreted as L-separated ion pair with water molecule(s) < L-separated one < w-shared one < contact one. When a cavity size of L is smaller than a size of M^+ , we will assume an opposite relation of $LM^+w-X^- < M^+L-X^-$; namely, M^+L-X^- approaches to LM^+-X^- . The relations, (R5) and (R7), seem to reflect the hydrophobic properties of ML^+ . The others can reflect simply effects of the sizes of the L skeletons with benzo groups.

4.1.3. Effect of ring sizes of L

Effect of the ring sizes of L in MLX is described and thereby its cause is examined. Also, this means an increase in the number of the O donor atoms in the ring. These K_{MLX}^0 relations in Table 5 are

$$L = 15C5 < 18C6 \text{ and } B15C5 < B18C6 \text{ for NaPic, KPic, NaMnO}_4, \text{ and NaBPh}_4 \quad (R10)$$

$$15C5 > 18C6 \text{ and } B15C5 > B18C6 \text{ for KMnO}_4 \text{ and AgPic.} \quad (R11)$$

Inequality (R10) can be interpreted as the following interactions of ML^+ with X^- : $Na^+(15C5)^- < (18C6)Na^+w-Pic^-$; $wK^+(15C5)^- < (18C6)K^+-Pic^-$; $Na^+(15C5)^- < (18C6)K^+w-X^-$ at $X^- = MnO_4^-$ and BPh_4^- . Similarly, interactions for (R10) may be $Na^+(B15C5)^- < (B18C6)Na^+-X^-$ at $X^- = Pic^-$ and MnO_4^- ; $wK^+(B15C5)^- < (B18C6)K^+-Pic^-$. On the other hand, Inequality (R11) seems to simply reflect a coulombic interaction between ML^+ with X^- .

4.1.4. Effect of sizes of the central M^{z+} in/on L rings

Effective ionic radii of M^+ are on the order $M^+ = Li^+ (0.76 \text{ \AA}) < Na^+ (1.02) < Ag^+ (1.15) < K^+ (1.38)$ [17]. Also, the hydration free energies ($-\Delta G_h^0$) of M^+ are on the order $K^+ (304 \text{ kJ mol}^{-1}) < Na^+ (375) < Li^+ (481) < Ag^+ (1856)$ [18]. The K_{MLX}^0 orders are

$$M = K < Na < Ag \text{ for } M(15C5)Pic \quad (O12)$$

$$K < Li < Na < Ag \text{ for } M(B15C5)Pic \quad (O13)$$

$$Li \leq Na < Ag < K \text{ for } M(18C6)Pic \quad (O14)$$

$$Ag < Na < K \text{ for } M(B18C6)Pic \quad (O15)$$

and

$$Na < K \text{ for } M(15C5)MnO_4 \quad (R16)$$

$K < Na$ for $M(B15C5)MnO_4$, $M(18C6)MnO_4$, and $M(B18C6)MnO_4$. (R17)

If the coulombic force is simply effective for these ion-pair formation, then the K_{MLX}^0 order can be $K^+ < Ag^+ < Na^+ < Li^+$. Similarly, if the dehydration of M^+ is effective for the formation, then the order can be $Ag^+ \ll Li^+ < Na^+ < K^+$. Comparison of these orders with (O12) to (O14) shows the complications of their ion-pair formation.

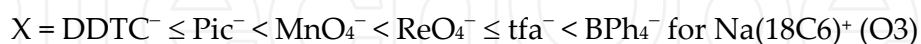
The orders or relations can be changed into $wK^+(15C5)^- \& (15C5)K^+w^- < Na^+(15C5)^- < (15C5)Ag^+w^- \& wAg^+(15C5)-Pic^-$ for Inequality (O12); $wK^+(B15C5)^- < Li^+(B15C5)^- < Na^+(B15C5)^- \& (B15C5)Na^+ < (B15C5)Ag^+-Pic^-$ for (O13); $wLi^+(18C6)^- \leq wNa^+(18C6)^- \& (18C6)Na^+w^- < (18C6)Ag^+w^- \& wAg^+(18C6)^- < (18C6)K^+ \& K^+(18C6)-Pic^-$ for (O14); $Ag^+(B18C6)^- < (B18C6)Na^+ < K^+(B18C6)-Pic^-$ for (O15) and $Na^+(15C5)^- < (15C5)K^+w^-MnO_4^-$ for (R16); $wK^+(B15C5)^- \& (B15C5)K^+w^- < Na^+(B15C5)^- \& (B15C5)Na^+MnO_4^-$; $K^+(18C6)^-$ and $(18C6)K^+ < (18C6)Na^+w^- \& wNa^+(18C6)-MnO_4^-$; $K^+(B18C6)^- < (B18C6)Na^+MnO_4^-$ for (R17). The above expression " $M^+L-X^- \& LM^+-X^-$ " means that the fraction of the left M^+L-X^- is major in comparison with that of the right LM^+-X^- .

In (O12), the inverse between $K(15C5)^+$ and $Na(15C5)^+$ is due to the fact that $K(15C5)^+$ satisfies the condition that the cavity size of 15C5 $<$ the size of K^+ (see 4.1.2); that between $Na(15C5)^+$ and $Ag(15C5)^+$ suggests that a fraction of $(15C5)Ag^+w-Pic^-$ is dominant. Further, the $Na(B15C5)^+ < Ag(B15C5)^+$ relation in (O13) suggests that Na^+ in the former complex ion is more shielded by B15C5 than Ag^+ in the latter ion. The same can be true of the relation of $Na(18C6)^+ < Ag(18C6)^+$ in (O14).

In the present section 4.1, the orders in magnitude among the K_{MLX}^0 values are interpreted by supposing the shapes of the MLX ion pairs based on Inequality (SO9). Of course, validity of such interpretations has to be clarified experimentally.

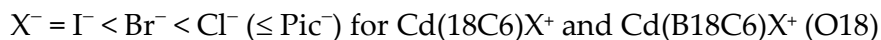
4.2. Try to understand the ion-pair formation based on the HSAB principle [8]

According to the HSAB classification, Pic^- , MnO_4^- , ReO_4^- , tfa^- , and BPh_4^- were reported to be hard bases [8]. Also, $DDTC^-$ has been classified as a soft base [19]. Then the K_{MLX}^0 values are on the orders



Here, only $DDTC^-$ has S donor atoms in it, while the other X^- does O donor atoms in them. The sequence of donor atoms in X^- obviously show $S \leq O < O < O < O$ (or F) for (O3) and $S < O < O$ (or F) $< O < O$ for (O4), except for $X^- = BPh_4^-$. Comparing the orders with those described in 3.4, they indicate at least that $Na(18C6)^+$ and $Na(B18C6)^+$ have the higher affinities for the O donor atoms in their X^- than the S donor ones in $DDTC^-$. This fact suggests that both the NaL^+ are classified as hard acids [8].

Similarly, from the following orders, readers can see that the same is true of the K_{CdLX}^0 values for the CdX^+-L systems with $X^- = Cl^-, Br^-,$ and I^- .



That is, it is suggested that both the complex ions are hard acids [8], although Cd^{2+} is classified as a soft acid (see 3.4); K_{CdX^0} is on the order $X^- = \text{Cl}^- \leq (\text{Pic}^- \leq) \text{Br}^- < \Gamma^-$ (see Table 5). As can be seen from the section 3.4 and the above, the facts that Cl^- and Pic^- are the hard bases support this suggestion

MX_z or M_2X	$K_{\text{MX}^0} [K_2^0], (\text{std})^a$	MLX_z	$K_{\text{MLX}_z^0} \{\beta_2^0\}, (\text{std})^a$
LiPic	10.9(1.8)	Li(B15C5)Pic	205(111)
		Li(18C6)Pic	52(--- ^b)
NaPic	4.2(0.7)	Na(15C5)Pic	34(6)
		Na(B15C5)Pic	517(91)
		Na(18C6)Pic	62(18)
		Na(B18C6)Pic	642(96)
KPic	5.8(1.8)	K(15C5)Pic	6.0(3.9)
		K(B15C5)Pic	12(--- ^b)
		K(18C6)Pic	738(210)
		K(B18C6)Pic	$1.37(0.12) \times 10^3$
AgPic	2.8(0.3)	Ag(15C5)Pic	556(68)
		Ag(B15C5)Pic	$1.58(0.21) \times 10^3$
		Ag(18C6)Pic	191(19)
		Ag(B18C6)Pic	157(22)
NaMnO ₄	8.0(0.9)	Na(15C5)MnO ₄	38(21)
		Na(B15C5)MnO ₄	354(75)
		Na(18C6)MnO ₄	231(30)
		Na(B18C6)MnO ₄	$1.63(0.41) \times 10^3$
KMnO ₄	9.1(2.3)	K(15C5)MnO ₄	239(80)
		K(B15C5)MnO ₄	137(110)
		K(18C6)MnO ₄	93(22)
		K(B18C6)MnO ₄	72(12)
Natfa	4.0(0.8)	Na(18C6)tfa	384(67)
		Na(B18C6)tfa	201(25)
NaReO ₄	4.1(0.7)	Na(18C6)ReO ₄	340(66)
		Na(B18C6)ReO ₄	188(112)
NaDDTC	32.8(2.7)	Na(18C6)DDTC	48(23)
		Na(B18C6)DDTC	100(25)
NaBPh ₄	14.3(1.5)	Na(15C5)BPh ₄	$7.36(1.51) \times 10^3$
		Na(B15C5)BPh ₄	$9.07(6.30) \times 10^3$
		Na(18C6)BPh ₄	$2.9(2.0) \times 10^5$
		Na(B18C6)BPh ₄	$1.24(1.02) \times 10^5$
CaCl ₂ [6]	40(7), 41(3)		
Ca(Pic) ₂ [6]	88(58)		

MX_z or M_2X	$K_{MX^0} [K_2^0], (\text{std})^a$	MLX_z	$K_{MLX_z^0} \{\beta_2^0\}, (\text{std})^a$
CdCl ₂	86(30), 92(4) [8.7(7.5), 13(5)]	Cd(18C6)Cl ₂	3.8×10^4 {1.39(1.00) $\times 10^6$ }
		Cd(B18C6)Cl ₂	1.7×10^4 , 2.70(2.48) $\times 10^6$
CdBr ₂	118(19) [25(19)]	Cd(18C6)Br ₂	0.57(0.13)
		Cd(B18C6)Br ₂	1.32(0.05)
CdI ₂	308(5) [40(3)]	Cd(18C6)I ₂ , Cd(B18C6)I ₂	< 1 ^c
Cd(Pic) ₂	108(11), 107(17)	Cd(18C6)(Pic) ₂	3.3×10^4 {1.77(1.62) $\times 10^7$ }
		Cd(B18C6)(Pic) ₂	6.5×10^4 {2.29(0.29) $\times 10^7$ }
CdSO ₄	221(31)	Cd(18C6)SO ₄	$4.38(0.68) \times 10^4$
		Cd(B18C6)SO ₄	$1.83(0.51) \times 10^4$
Na ₂ SO ₄	14(0.7) [7.4(1.0)]		
Na ₂ S ₂ O ₃	14(0.6) [3.2(0.6)]		
Na ₂ CrO ₄	12(2) [7.9(2.8)]		

a. Standard deviation or standard errors.

b. See Appendix B in Ref. [14].

c. Estimated from experimental results in Ref. [8].

Table 5. Ion-pair formation constants of MX_z , M_2X , and MLX_z in water at $I \rightarrow 0 \text{ mol dm}^{-3}$ and 25 °C [4-8,12,14]

5. Topics relevant to the ion-pair formation in water

5.1. Application to solvent extraction [20]

Using the thus-determined formation constants for M^+X^- and M^+L in water, overall extraction equilibrium-constants are resolved into the following component ones [21].



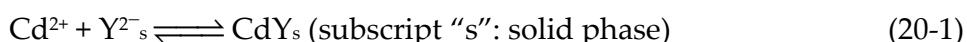
and



Here, the subscript "o" denotes an organic phase. The reactions (19-1) to (19-5) correspond to the extraction into low polar diluents (or organic solvents) and the reaction (19-6) will be added to the cases of the extraction into high polar diluents. In general, the equilibrium constants of the process (19-1) and the reaction (19-3) can be determined by separate experiments. Then, the overall extraction equilibria are characterized on the basis of their component ones, either (19-1) to (19-5) or to (19-6). One can clearly see that, for the above extraction model, the ion-pair formation, (19-2) and (19-4), is important. The NaMnO_4 extraction by B15C5 into 1,2-dichloroethane (DCE) and nitrobenzene (NB) are analyzed as the results in Table 6. There are remarked differences in $K_{D,\text{NaLX}}$, $K_{D,X}$, and $K_{\text{NaLX}^{\text{org}}}$ between DCE and NB. According to the relation $K_{\text{ex}} = K_{\text{ML}}K_{\text{MLX}}K_{D,\text{MLX}}/K_{D,L}$ [21], a difference in K_{ex} between NB and DCE mainly comes from that between $K_{D,\text{MLX}}$. Similarly, that between $K_{\text{ex}\pm}$ does from the difference between $K_{\text{MLX}^{\text{org}}}$ in addition to $K_{D,\text{MLX}}$, because $K_{\text{ex}\pm} = K_{\text{ex}}/K_{\text{MLX}^{\text{org}}}$.

5.2. Development into study of the abnormal potential responses of ISEs [9]

Abnormal potential responses, Λ -shaped potential ones [9,12] of emf-versus-log $[\text{CdX}_2]_t$ plots ($X = \text{I}, \text{Br}$), of the commercial Cd^{2+} -selective electrode listed in Table 1 have been observed and then an answer is described using a model for the potential response with interactions of the electrode surface with counter X^- , in addition to that with Cd^{2+} . Its processes are



where Y^{2-}_s is a functional group of the electrode material and X^- denotes halide ions. Applying electrochemical potentials [2] for the electrode processes (20-1) and (20-2) and introducing mass-balance equations in the overall process, we obtain the following equation as an expression of emf.

$$\text{emf} = A + B \log [\text{Cd}]_t + C \log \{1 + 4K_s([\text{Cd}]_t)^2\} \quad (21)$$

Here, A , $[\text{Cd}]_t$, B , C , and K_s refer to a constant (V versus $\text{Ag}|\text{AgCl}$ electrode), the total concentration of CdX_2 in the test solution, values (V) corresponding to $-2.3RT/2F$, and value ($\text{mol}^{-3} \text{dm}^9$ unit) being inversely proportional to the solubility product of CdX_2 , respectively. One can immediately obtain these values, analyzing the plot of emf versus $\log [\text{Cd}]_t$ by non-linear regression: $K_s(\text{CdCl}_2)$ (not be determined) $< K_s(\text{CdBr}_2)$ ($= 10^{4.2} \text{ mol}^{-3} \text{ dm}^9$) $< K_s(\text{CdI}_2)$ ($= 10^{6.98}$) [8]. It is obvious that the larger K_s is, the more easy CdX_2 interacts with the electrode and accordingly the larger the interference of X^- against the electrode response becomes. Similar tendencies have been obtained in a commercial Cu^{2+} -selective electrode with a solid membrane and a Ca^{2+} -selective one with a liquid membrane.

Diluent	$\log K_{ex}^a$	$\log K_{ex\pm}^b$	$\log K_{ML}^c$	$\log K_{MLX}$	$\log K_{MX}$	$\log K_{D,MLX}^e$	$\log K_{D,L}^f$	$\log K_{D,X}^g$	$\log K_{MLX}^{org\ h}$
				(I) ^d					(I _o) ⁱ
DCE	2.24	-3.7 ₅	0.45	2.47 (0.0084)	0.54	1.23	1.910	-3.3	6.0 (4.5 × 10 ⁻⁶)
NB	3.79	-0.2 ₃	0.45	2.51 (0.0015)	0.59	2.4	1.6	-1.7	4.0 (3.5 × 10 ⁻⁵)

a. Defined as $K_{ex} = [MLX]_o/[M^+][L]_o[X^-]$. b. Defined as $K_{ex\pm} = [ML^+]_o[X^-]_o/[M^+][L]_o[X^-]$. c. As $K_{ML} = [ML^+]/[M^+][L]$. d. Ionic strength in a water phase. e. As $K_{D,MLX} = [MLX]_o/[MLX]$. f. As $K_{D,L} = [L]_o/[L]$. g. As $K_{D,X} = [X^-]_o/[X^-]$. h. Estimated from $K_{MLX}^{org} = K_{ex}/K_{ex\pm}$. i. Ionic strength in the o phase.

Table 6. Extraction constants and their component equilibrium-constants for the NaMnO₄-B15C5 extraction systems into DCE and NB at 25 °C [20]

6. Summary

In this chapter, the determination procedures of the K_{MXz}^0 , K_{M2X}^0 , and K_{MLXz}^0 values in water were discussed and their some applications were described. The present potentiometric procedures will support other methods, such as conductometric, spectrophotometric, solvent extraction ones, and so on. Their applications have been limited to some ions and hydrophilic L, because kinds of commercial ISE is limited and low solubility of hydrophobic L to water limits its emf measurements; the solvent extraction method [21] is going to compensate for the latter limitation. Instead of such situations, the present procedures are useful for the K_{MLXz}^0 determination. As the pH values are measured at many laboratories in the world, thus handy procedures, compared with the other methods, will take effect at the determination of K_{MXz} and K_{MLXz} at $I \rightarrow 0$.

Author details

Yoshihiro Kudo
Chiba University, Japan

Appendix

Symbols and abbreviations used in this chapter

Symbol and abbreviation	Meaning
$a(j)$	Ion size parameter of j
B15C5	Benzo-15-crown-5 ether
B18C6	Benzo-18-crown-6 ether
c_j^I or c_j^{II}	Molar concentration of j in the phase I or II
DDTC ⁻	Diethyldithiocarbamate ion
DME	Dropping mercury electrode
E_j	Liquid junction potential at an interface
$I \rightarrow 0$	Ionic strength at infinite dilution
$[j]$	Molar concentration of j at equilibrium
$[j]_t$	Total concentration of j

K	The equilibrium constant
Pic^-	Picrate ion
R	Correlation coefficient
RT/F	0.02569 V at 298 K
tfa	Trifluoroacetate ion
u_j	Mobility of j in water
z	Formal charge of an ion or a number expressing the composition of a salt or an ion pair
z_j	Formal charge of j
ϕ^I or ϕ^{II}	Inner potential in the phase I or II
$2.3RT/F$	0.05916 V at 298 K

7. References

- [1] G. D. Christian, *"Analytical Chemistry"*, 5th ed., John Wiley & Sons, New York, 1994.
- [2] A. J. Bard and L. R. Faulkner, *"Electrochemical Methods: Fundamentals and Applications"*, 2nd ed., John Wiley & Sons, New York, 2001.
- [3] S. Katsuta, H. Wakabayashi, M. Tamaru, Y. Kudo, and Y. Takeda, *J. Solution Chem.*, 2007, 36, 531.
- [4] Y. Kudo, M. Wakasa, T. Ito, J. Usami, S. Katsuta, and Y. Takeda, *Anal. Bioanal. Chem.*, 2005, 381, 456.
- [5] Y. Kudo, R. Fijihara, T. Ohtake, M. Wakasa, S. Katsuta, and Y. Takeda, *J. Chem. Eng. Data*, 2006, 51, 604.
- [6] Y. Kudo, S. Takeuchi, Y. Kobayashi, S. Katsuta, and Y. Takeda, *ibid.*, 2007, 52, 1747.
- [7] Y. Kudo, Y. Kobayashi, S. Katsuta, and Y. Takeda, *J. Mol. Liquids*, 2009, 146, 60.
- [8] Y. Kudo, T. Koide, Y. Zhao, S. Katsuta, and Y. Takeda, *Anal. Sci.*, 2011, 27, 1207.
- [9] Y. Kudo, D. Todoroki, N. Suzuki, N. Horiuchi, S. Katsuta, and Y. Takeda, *Amer. J. Anal. Chem.*, 2011, 2, 9.
- [10] J. Kielland, *J. Am. Chem. Soc.*, 1937, 59, 1675.
- [11] P. Vanýsek, *"Ionic Conductivity and Diffusion at Infinite Dilution"* in *"CRC Hand Book of Chemistry and Physics"*, ed. D. R. Lide, 74th ed., CRC Press, Boca Raton, 1993.
- [12] Y. Kudo, D. Todoroki, N. Horiuchi, S. Katsuta, and Y. Takeda, *J. Chem. Eng. Data*, 2010, 55, 2463.
- [13] R. de Levie, *"Aqueous Acid-Base Equilibria and Titration"*, ed. R. G. Compton, Oxford Chemistry Primers 80, Oxford University Press, New York, 1999.
- [14] Y. Kudo, J. Usami, S. Katsuta, and Y. Takeda, *J. Mol. Liquids*, 2006, 123, 29.
- [15] R. G. Pearson, *J. Chem. Educ.*, 1968, 45, 581.
- [16] R. G. Pearson, *Inorg. Chim. Acta*, 1995, 240, 93.
- [17] R. D. Shannon, *Acta Crystallogr.*, 1976, A32, 751.
- [18] Y. Marcus, *"Ion Properties"*, Marcel Dekker Inc., New York, 1997.
- [19] H. Kawamoto and H. Akaiwa, *Chem. Lett.*, 1990, 1451.
- [20] Y. Kudo, K. Harashima, S. Katsuta, and Y. Takeda, *International J. Chem.*, 2011, 3, 99.
Y. Takeda, R. Taguchi, and S. Katsuta, *J. Mol. Liquids*, 2004, 115, 139.